



Hyper-diversity of CRH interneurons in mouse hippocampus

Benjamin G. Gunn¹ · Gissell A. Sanchez² · Gary Lynch³ · Tallie Z. Baram^{1,2} · Yuncai Chen^{1,2}

Received: 18 June 2018 / Accepted: 9 November 2018 / Published online: 20 November 2018
© Springer-Verlag GmbH Germany, part of Springer Nature 2018

Abstract

Hippocampal inhibitory interneurons comprise an anatomically, neurochemically and electrophysiologically diverse population of cells that are essential for the generation of the oscillatory activity underlying hippocampal spatial and episodic memory processes. Here, we aimed to characterize a population of interneurons that express the stress-related neuropeptide corticotropin-releasing hormone (CRH) within existing interneuronal categories through the use of combined electrophysiological and immunocytochemical approaches. Focusing on CA1 strata pyramidale and radiatum of mouse hippocampus, CRH interneurons were found to exhibit a heterogeneous neurochemical phenotype with parvalbumin, cholecystokinin and calretinin co-expression observed to varying degrees. In contrast, CRH and somatostatin were never co-expressed. Electrophysiological categorization identified heterogeneous firing pattern of CRH neurons, with two distinct subtypes within stratum pyramidale and stratum radiatum. Together, these findings indicate that CRH-expressing interneurons do not segregate into any single distinct subtype of interneuron using conventional criteria. Rather our findings suggest that CRH is likely co-expressed in subpopulations of previously described hippocampal interneurons. In addition, the observed heterogeneity suggests that distinct CRH interneuron subtypes may have specific functional roles in the both physiological and pathophysiological hippocampal processes.

Keywords Hippocampus · Interneuron · CRH · Stress

Introduction

The hippocampus is a brain region essential for spatial and episodic memory (Neves et al. 2008). Such cognitive processes are believed to be influenced by different types of oscillatory activity (e.g., theta, beta and gamma rhythms) that occur within the hippocampus during specific behavioral events (Colgin 2016). The generation of hippocampal, and indeed brain oscillations, reflects the highly coordinated activity of principal cells that are maintained by inhibitory GABAergic interneurons (Cobb et al. 1995; Freund and

Buzsaki 1996; Bartos et al. 2007; Klausberger and Somogyi 2008). During oscillatory activity, specific interneurons, of which there are at least 20 distinct types within the hippocampus, innervate discrete subcellular regions (e.g., soma, dendrites, axon initial segment) of pyramidal cells in a temporally distinct manner (Klausberger and Somogyi 2008). Importantly, this spatio-temporal innervation of pyramidal cells by interneurons results in the activation of specific GABA_A receptor (GABA_AR) isoforms, which reside at discrete subcellular domains (i.e., synaptic or extrasynaptic sites) and are responsible for mediating phasic or tonic inhibition (Farrant and Nusser 2005). As such, this spatio-temporal innervation ensures that inhibitory transmission not only contributes to dampening pyramidal cell excitability, but can modulate the gain, spike timing and bursting properties of principal cells, as well as contributing to the selective filtering of dendritic inputs (Miles et al. 1996; Isaacson and Scanziani 2011; Lovett-Barron et al. 2012; Royer et al. 2012; Hu et al. 2014; Roux and Buzsaki 2015). Given the diversity of functions performed by interneurons, understanding how these inhibitory networks are organized, in particular whether specific rules govern their organization, remains a

✉ Tallie Z. Baram
tallie@uci.edu

✉ Yuncai Chen
yuncaic@uci.edu

¹ Department of Anatomy and Neurobiology, University of California-Irvine, Irvine, CA 92697-4475, USA

² Department of Pediatrics, University of California-Irvine, Irvine, CA 92697-4475, USA

³ Department of Psychiatry and Human Behavior, University of California-Irvine, Irvine, CA 92697-4475, USA

central issue. Classifying hippocampal interneurons based upon a combination of their laminar location and innervation as well as their neurochemical and electrophysiological properties has proved a useful framework (Freund and Buzsáki 1996; Klausberger and Somogyi 2008). Indeed, using such an approach, in vivo electrophysiological studies have indicated specific functional roles for these different interneuron subtypes during hippocampal oscillations, where action potential firing occurs at a distinct phase(s) of the oscillation (Klausberger et al. 2003, 2004; Klausberger and Somogyi 2008). However, when additional factors such as transmitter release probability, short-term plasticity (Toth et al. 2000), receptor expression (Mody and Pearce 2004), and neurochemical content (i.e., co-expression of multiple peptides) are considered, it has become increasingly apparent that such a classification framework may not suffice to categorize interneurons into single subtypes (Cossart et al. 2006; Tricoire et al. 2011).

Corticotropin-releasing hormone (CRH), a peptide classically associated with the neuroendocrine response to stress, is expressed in a population of interneurons located throughout the hippocampal layers (Yan et al. 1998b; Chen et al. 2001, 2004). Interestingly, electron microscopy studies suggest that these CRH-expressing interneurons do not represent a uniform population when the anatomical and neurochemical parameters typically used to define interneurons are considered (Yan et al. 1998b). The principal receptor for this peptide, CRH receptor 1 (CRHR1), resides at specific subcellular locations on pyramidal cells (Chen et al. 2000), while CRH receptor 2 (CRHR2) is restricted to the axon initial segment of these neurons (Joels and Baram 2009). Electrophysiological studies have demonstrated that within the hippocampus both exogenous and endogenously released CRH, primarily increases pyramidal cell excitability via multiple mechanisms including the inhibition of Ca^{2+} -dependent K^+ channel function (Aldenhoff et al. 1983; Haug and Storm 2000; Gunn et al. 2017) and attenuating A-type K^+ channel activation (Kratzer et al. 2013). CRH is rapidly released within the hippocampus following stress and this peptide has been implicated in mediating some of the stress-induced effects upon hippocampal function (Chen et al. 2004, 2010). The development of a number of transgenic reporter mouse lines that specifically target the *Crh* gene (Sarkar et al. 2011; Chen et al. 2015; Hooper and Maguire 2016; Kono et al. 2017) have allowed the visual identification of these interneurons and studies have begun to postulate the functional role(s) of these cells (Hooper and Maguire 2016; Hooper et al. 2018). Here, we employ a combined electrophysiological and immunocytochemical approach to characterize the properties of CRH-expressing interneurons located in strata pyramidale and radiatum of the mouse hippocampus CA1. Our data indicate that, based upon their electrophysiological and neurochemical

phenotype, CRH-expressing interneurons comprise distinct and heterogeneous populations both within str. pyramidale, and similarly in str. radiatum. These observations suggest that CRH interneurons may have functionally distinct roles in modulating hippocampal activity during physiological and possibly pathophysiological contexts.

Materials and methods

Animals

Male C57BL/6J mice as well as tdTomato-Crh (*Crh-IRES-Cre; Ai14*) transgenic mice were used in the experiments. In accord with recent NIH guidelines for rigor and reproducibility, we have aimed to conduct experiments that will yield robust, unbiased results. All procedures were performed in accordance with the National Institute of Health Guide for Care and Use of Laboratory Animals and were approved by the Institutional Care and Use Committee of the University of California, Irvine (UCI).

To generate tdTomato-Crh mice, B6(Cg)-Crh^{tm1(cre)Zjh/J} (*Crh-IRES-Cre*) and B6.Cg-Gt(ROSA)26Sor^{tm14(CAG-TdTomato)Hze/J} (*Ai14*) mice, obtained from Jackson laboratories (stock number 012704 and 007914, respectively), were maintained as homozygous colonies. Female homozygous *Crh-IRES-Cre* and male *Ai14* mice were mated and the resulting offspring (tdTomato-Crh) were used for subsequent experiments. Mice were group housed on a 12:12 light/dark cycle and provided with access to water and standard rodent chow ad libitum. Electrophysiological recordings were made from animals derived from at least three different litters. A total of 45 tdTomato transgenic mice (P21–P40) were used for whole-cell patch-clamp recordings and 24 C57BL/6J mice (3–4 months) used for immunocytochemistry.

Antibody characterization

The antibodies used in this study are described below and in the antibody table (Table 1). For CRH, this was a rabbit anti-human/rat CRH antiserum (Code #PBL rC68) provided as a gift from the antiserum resource center, Dr. Paul E. Sawchenko, Director, Salk Institute, La Jolla, CA, USA. The antiserum had been adsorbed with 2 mg human α -globulin and 1 mg α -MSH per ml serum. Detailed assessment of its specificity has been described (Chen et al. 2015).

Tissue preparation and immunohistochemistry (ICC)

Mice were anesthetized under stress-free conditions with sodium pentobarbital (40 mg/kg). This approach prevented stress-induced release of native CRH from somata to axons and obviated the need for colchicine. Mice were

Table 1 Primary antibodies used in the study

Antibody	Immunogen	Manufacturer, host, type	Dilution
Anti-CRH	Human/rat CRH	Provided by Paul E. Sawchenko, Salk Institute; rabbit polyclonal	1:20,000–40,000
Anti-GAD67	Mouse GAD67 (amino acids 87–106)	Sigma (G5419), mouse monoclonal (clone K-87)	1:2000
Anti-PV	Parvalbumin (PV) purified from frog muscle	Chemicon (MAB1572), mouse monoclonal (clone PARV-19)	1:10,000
Anti-CCK	Cholecystokinin (CCK)/gastrin	CURE/Digestive Disease Research Center, Antibody/RIA Core, UCLA; mouse monoclonal	1:2000
Anti-calretinin	Recombinant rat calretinin	Chemicon (MAB1568), mouse monoclonal (clone 6B8.2)	1:5000
Anti-somatostatin	Synthetic peptide corresponding to amino acids 1–14 of cyclic somatostatin conjugated to bovine thyroglobulin using carbodiimide	Chemicon (MAB354), rat monoclonal (clone YC7)	1:2000
Anti-calbindin D28k	<i>E. coli</i> -derived recombinant human calbindin D Met1-Asn261	ThermoFisher (MA5-24135), mouse monoclonal (clone 401025)	1:8000
Anti-RFP	RFP fusion protein corresponding to the full-length amino acid sequence (234aa) derived from the mushroom polyp coral <i>Discosoma</i>	Rockland (600-401-379), rabbit polyclonal	1:2000

transcardially perfused via the ascending aorta with 0.9% saline solution followed by perfusion with 4% paraformaldehyde solution made in 0.1 M phosphate buffer (PB, pH 7.4, 4 °C). Brains were postfixed in the perfusion-used fixative for 2–4 h (4 °C) and immersed in 15%, followed by 25% sucrose for cryoprotection. Brains were blocked in the coronal or sagittal planes and sectioned at 20 µm thickness using a cryostat. In each plane, 1 in 10 serial sections were subjected to CRH-ICC and an adjacent series of sections was stained with cresyl violet or DAPI (4',6-diamidino-2-phenylindole). The others were used for double labeling ICC.

CRH-ICC was performed on free-floating sections using standard avidin–biotin complex methods, as described previously (Chen et al. 2001). Briefly, after several washes with PBS containing 0.3% Triton X-100 (PBS-T, pH 7.4), sections were treated with 0.3% H₂O₂/PBS for 30 min, then blocked with 5% normal goat serum (NGS) for 30 min to prevent non-specific binding. After rinsing, sections were incubated for 2 weeks at 4 °C with rabbit anti-CRH antiserum (1:40,000) (Table 1) in PBS containing 1% BSA, and washed in PBS-T (3 × 5 min). Sections were incubated with biotinylated goat-anti-rabbit IgG (1:400, Vector laboratories, Burlingame, CA) in PBS for 2 h at room temperature. After washing (3 × 5 min), sections were incubated with the avidin–biotin–peroxidase complex solution (1:200, Vector) for 3 h, rinsed (3 × 5 min), and reacted with 0.04% 3,3'-diaminobenzidine (DAB) containing 0.01% H₂O₂.

Concurrent immunolabeling of CRH and somatostatin or calbindin D-28 was performed as described in detail previously (Chen et al. 2001, 2015). Briefly, sections were first incubated for 2 weeks at 4 °C with rabbit anti-CRH antiserum (1:40,000) in PBS containing 1% BSA, yielding a diffuse brown DAB reaction product. Sections were then rinsed

in PBS-T, preincubated in 5% NGS and exposed to mouse anti-somatostatin (1:2000) or anti-calbindin D28k antibodies (1:8000, ThermoFisher) 2 days at 4 °C, followed by the biotinylated second antibody and avidin–biotin–peroxidase complex solutions as described above. To visualize somatostatin or calbindin antibody binding, sections were rinsed, transferred to a 1 × acidic buffer (pH 6.2), and then incubated in reaction buffer containing benzidine dihydrochloride (BDHC) and H₂O₂ (Bioenno Tech, Santa Ana, CA, USA) for 5–6 min. The reaction stopped by rinsing in 0.01 M PB containing 0.1% Triton X-100 (pH 6.2).

Immunofluorescence single and dual staining

CRH immunofluorescence staining was performed on free-floating sections using the tyramide signal amplification (TSA) technique (Chen et al. 2004). Sections were incubated with CRH rabbit antiserum (1:20,000) for 5–6 days (4 °C), then treated with HRP conjugated anti-rabbit IgG (1:1000; Perkin Elmer, Boston, MA, USA) for 1.5 h. Fluorescein or cyanine 3-conjugated tyramide was diluted (1:150) in amplification buffer (Perkin Elmer, Boston, MA, USA), and was applied in dark on ice for 5–6 min. To visualize the dendritic spines on pyramidal-like tdTomato cells in the hippocampus, free-floating sections were incubated with rabbit anti-RFP (1:2000) overnight at 4 °C, followed by incubating in anti-rabbit IgG conjugated to Alexa Fluor 488 or 568 (1:400, Invitrogen) for 2 h (RT).

To assess the co-expression of potentially low levels of CRH in tdTomato reporter-expressing neurons, concurrent visualization of CRH peptide and tdTomato was performed using the TSA technique as described. For dual labeling of CRH and parvalbumin (PV), cholecystokinin (CCK) or

calretinin, sections were first incubated with CRH (1:20,000) as described above, yielding a green or red fluorescence reaction product. Following CRH detection, sections were then rinsed in PBS-T, preincubated in 5% NGS and exposed to GAD67 (1:2000), PV (1:10,000), CCK (1:2000) or calretinin (1:5000) antibodies for 2 days at 4 °C. Immunoreactivity was visualized using anti-mouse or anti-rat IgG conjugated to Alexa Fluor 488 or 568 (1:400, Invitrogen).

Combined in situ hybridization (ISH) and ICC

Combined ISH and ICC were performed as described previously (Chen et al. 2001). Briefly, free-floating sections were first processed for GAD67-ISH followed by CRH-ICC: for hybridization, DIG-labeled RNA probes were added, and sections were incubated overnight at 55 °C. Following hybridization, sections were washed, most stringently in $0.1 \times \text{SSC}$ at 65 °C for 30 min, and hybrid molecules were detected using an anti-DIG-alkaline phosphatase. For visualization of CRH-immunoreaction, sections were rinsed and processed for CRH-ICC as above with the exception that decreased concentrations of DAB (0.02%) and H_2O_2 (0.005%) were used. The specificity of the hybridization reaction was verified by substituting labeled sense probe for the antisense probe and by omitting either the antisense probe or alkaline phosphatase-conjugated antibody. No labeling was observed under these conditions. To evaluate the possibility of altered sensitivity or specificity due to combined ISH/ICC, sections processed only for ICC or ISH were compared with matched sections subjected to the dual procedure.

Electrophysiology

Brain slice preparation

Hippocampal brain slices were prepared from male tdTomato-Crh mice (PND 21–40). Briefly, brains were rapidly removed and placed in ice cold, oxygenated (95% O_2) artificial CSF (aCSF) containing (in mM): 87 NaCl, 75 sucrose, 26 NaHCO_3 , 2.5 KCl, 1.25 NaH_2PO_4 , 0.5 CaCl_2 , 7 MgCl_2 and 10 glucose (320–335 mOsm). Coronal brain slices (300–320 μm) were then cut using a vibratome (Leica VT 1000) at 0–4 °C. Slices were subsequently incubated in a recovery chamber at room temperature for up to 1 h in oxygenated aCSF (as above), before being transferred to a holding chamber and incubated at room temperature (20–22 °C) in oxygenated extracellular solution (ECS) containing (in mM): 124 NaCl, 3 KCl, 1.25 NaH_2PO_4 , 2.5 CaCl_2 , 1.25 MgSO_4 , 26 NaHCO_3 , and 10 glucose (300–310 mOsm, pH ~ 7.4). Slices were then transferred to the recording chamber as required.

Whole-cell current-clamp recordings

Neurons were visualized with an upright microscope fitted with epifluorescence optics (Nikon Eclipse FN1) and camera (Photometrics CoolSNAP MYO). Fluorescent neurons with a more pyramidal shape that were found not to co-express CRH (Fig. 2d–i) were not targeted for electrophysiology. Spontaneous and evoked action potentials were recorded from CRH interneurons at 26–28 °C in ECS (as above), using patch pipettes ($R = 5\text{--}8 \text{ M}\Omega$) filled with an intracellular (IC) solution containing the following (in mM): 135 K-glucuronate, 10 HEPES, 4 KCl, 1 MgCl_2 , 2 Mg-ATP, 0.3 Na-GTP and 10 Tris-phosphocreatine, 300–310 mOsm, pH 7.2–7.3 with KOH. The IC solution additionally contained 1 mg/ml neurobiotin to label the recorded neuron for post hoc analysis. Within the CA1, CRH interneurons and pyramidal cells were held at an uncorrected (for liquid junction potential) membrane potential of –60 to –65 mV and incremental 10 pA current steps (500 ms duration) were injected every 10 s (from –40 to 100 pA). For recordings of spontaneous action potentials and intrinsic physiological properties a liquid junction potential of 14 mV was corrected as previously described (Neher 1992). Currents were filtered at 5 kHz using an 8-pole low-pass Bessel filter. All recordings were performed using an Axopatch 1D amplifier (Molecular Devices) and pClamp 9. Recordings were stored directly to a PC (10 kHz digitization) using a Digidata 1322A (Molecular Devices) for analysis offline.

At the end of recordings, slices were collected into 4% paraformaldehyde in 0.1 M phosphate buffer (PB, pH 7.4, 4 °C) and fixed 60 min for post hoc analysis of recorded cells. The fixed slices were cryoprotected and sub-sectioned (25 μm). CRH-neurobiotin dual-labeling ICC was performed on free-floating sections. Briefly, CRH was detected using the tyramide signal amplification (TSA) technique as described above. The neurobiotin signal was visualized with avidin conjugated to Alexa Fluor 488 (1:400; Invitrogen).

Imaging

Brain sections were visualized on a Nikon Eclipse E400 epi-fluorescence microscope equipped with fluorescein, rhodamine, and DAPI/FITC/TRITC filter sets. Light microscope images were obtained using a Nikon Digital Sight camera controlled by NIS-Elements F software (version 3.0, Nikon Instruments Inc., Melville, NY, USA). Confocal images were taken using an LSM 510 confocal microscope (Zeiss, Göttingen, Germany) with an Apochromat 63 \times oil objective (numeric aperture = 1.40). Virtual z-sections of < 1 μm were taken at 0.2–0.5 μm intervals. Image frame was digitized at 12 bit using a 1024 \times 1024 pixel frame size. To prevent bleed-through in dual-labeling experiments, images were scanned sequentially (using the “multi-track” mode)

by two separate excitation laser beams: an argon laser at a wavelength of 488 nm and a He/Ne laser at 543 nm. Z-stack reconstructions and final adjustments of image brightness were performed using ImageJ software (version 1.43, NIH).

A square lattice system placed over str. pyramidale and str. radiatum of hippocampus CA1, was used to quantify (i.e., count) the number of immunofluorescent cells present. A first-pass analysis was conducted using a 20 × magnification, which was further verified under a higher 63 × magnification. For each animal, 5–6 sections per hippocampus were analyzed, and a total of six mice used to calculate the final cell numbers and overlap ratios.

Data analysis

Action potentials were detected in Clampfit 10.2 using an amplitude threshold algorithm and visually inspected for validity. Action potentials were analyzed with regard to their amplitude (total spike), rise time (10–90%), decay time (10–90%), half-width and the amplitude of the after-hyperpolarization (AHP). An input–output (I – O) curve determining the number of action potentials fired in response to current injection was measured and the output calculated as events per second (i.e., Hz) for each cell. The action potential threshold was defined as the voltage at which the upward slope reached 10 mV/ms following a current injection (differed across cells). The rheobase for each cell was defined as the current injection that elicited 3 or more action potentials. A neuron is typically considered as fast spiking if the firing frequency is > 50 Hz at RT (22 °C) and > 150 Hz at physiological temperature (35 °C, Hu et al. 2014). Using an estimated Q_{10} value of 2.3, in the present study (temp 26–28 °C) a neuron was considered fast-spiking if the action potential frequency was > 58 Hz. The current–voltage (I – V) relationship was calculated at an uncorrected membrane potential of –60 to –65 mV for each current step (from –40 to +50 pA) and a mean input resistance (R_{input}) calculated as the change in voltage following a –10 pA current injection (Ohm's law: resistance [R] = voltage [V]/current [I]). In general, at least three stimulation protocols/cell was used to calculate the mean I – O , I – V and R_{input} values. The resting membrane potential was measured by averaging a section(s) of stable, event free baseline recording. The membrane time constant (τ_{membrane}) was determined by fitting a single exponential function to the first 250 ms of the voltage response induced by a –10 pA current step (500 ms).

Statistical analysis

Data were analyzed using Prism 6 software (GraphPad Prism, RRID: SCR_002798, San Diego, CA, USA). Tests included one-way or two-way analysis of variance (ANOVA) as indicated in the text, with Bonferroni's or Newman–Keuls

post hoc tests. Significance was set at 95% confidence, and values are presented as mean \pm SEM unless otherwise indicated.

Results

CRH expressing neurons are exclusively GABAergic

In the hippocampus, CRH-immunoreactive (ir) neurons were distributed throughout all layers of hippocampal subregions. In area CA1, CRH-ir cells typically had a small round or fusiform soma with short primary dendrites and were primarily located in the pyramidal cell layer and stratum radiatum (Fig. 1). Consistent with previous studies (Yan et al. 1998b), these CRH-ir cells are GABAergic interneurons. They co-expressed glutamate decarboxylase 67 (GAD_{67}) mRNA (Fig. 1a, b) and protein (Fig. 1c–e; Table 2), representing ~7% of GAD_{67} mRNA-expressing interneurons (Table 2). To confirm the validity of a tdTomato-Crh mouse line, we used dual labeling immunocytochemistry to check the expression of *Crh* reporter and its colocalization with endogenous CRH peptide (Fig. 2). We found tdTomato reporter-expressing cells located throughout the hippocampal layers (Fig. 2d). In the pyramidal cell layer and stratum radiatum, the large majority of reporter-expressing cells co-expressed CRH peptide (Fig. 2a–c). We did observe reporter expression without co-expression of CRH in a population of pyramidal-like cells (Fig. 2d–i). These large cells were typically located towards the border of CA1 and CA3 (Fig. 2d) and were morphologically similar to pyramidal cells (Fig. 2e, f). Indeed, the observation that these neurons have abundant spines located on the apical dendrites (Fig. 2e, f) lends support to the notion that they are in fact pyramidal cells. The absence of CRH expression in these large pyramidal-like neurons was in contradistinction to the clear CRH co-expression observed in neighboring non-pyramidal like cells within the same section (Fig. 2g–i). These findings corroborate previous characterizations of this mouse line (Chen et al. 2015), and, despite a degree of non-specific reporter labeling (e.g., pyramidal-like cells, dentate gyrus granule cells), highlight its value as a potential tool for exploring the properties of these neurons (see “Discussion”).

CRH interneurons in the pyramidal cell layer and stratum radiatum are neurochemically heterogeneous

We next investigated the neurochemical phenotype of CRH interneurons to further characterize this population of cells. Using dual-labeling immunocytochemistry, we identified and quantified the number of CRH-interneurons within the pyramidal cell layer and str. radiatum of area CA1 that

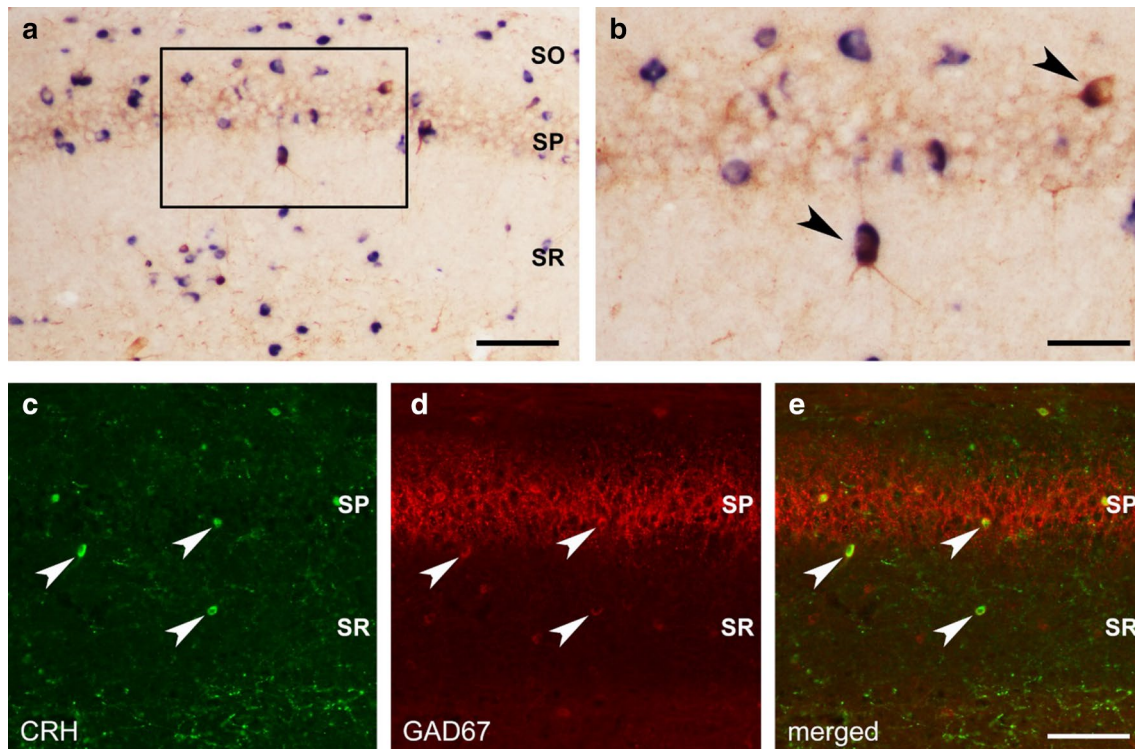


Fig. 1 Endogenous CRH was exclusively expressed in GABAergic interneurons in strata pyramidale and radiatum of hippocampal area CA1 of adult C57BL/6J mice. CRH-immunoreactive (ir) somata co-expressed the GABA synthesizing enzyme glutamic acid decarboxylase GAD67 at both mRNA (**a, b**) and protein (**c–e**) levels, using combined immunohistochemistry and in situ hybridization (CRH,

brown; GAD67 mRNA, blue) as well as dual labeling immunofluorescence (CRH, green; GAD67, red), respectively. The colocalization was denoted by arrowhead. SO, stratum oriens; SP, stratum pyramidale; SR, stratum radiatum. Scale bars 100 μm (**a**), 45 μm (**b**), and 125 μm (**c–e**)

Table 2 Colocalization of CRH and other interneuron markers in str. pyramidale and radiatum of field CA1

	Str. Pyramidale	Str. Radiatum
GAD ₆₇ –CRH/CRH	100 \pm 0 ^a (562) ^b	94.91 \pm 0.68 (436)
GAD ₆₇ –CRH/GAD ₆₇	6.56 \pm 0.22 (4450)	6.88 \pm 0.42 (3008)
PV–CRH/CRH	42.76 \pm 1.36 (548)	4.57 \pm 2.10 (417)
CCK–CRH/CRH	16.39 \pm 1.57 (429)	33.90 \pm 1.78 (372)
Calretinin–CRH/CRH	25.79 \pm 1.20 (527)	21.01 \pm 1.54 (425)
Somatostatin–CRH/CRH	0 (452)	0 (395)
Calbindin D-28–CRH/CRH	0 (401)	0 (352)

The quantitative analysis was performed on series sections from 5 mice, $n = 5$

^aValues represent % of dual-labeled cells \pm SEM

^bNumber in () represents CRH-ir cells or GAD₆₇ mRNA-expressing cells counted in the defined layer

co-expressed parvalbumin (PV), cholecystokinin (CCK), calretinin (CR), somatostatin (SOM) and calbindin D-28 (CB). Among these interneurons, PV was almost exclusively co-expressed with CRH interneurons located within str. pyramidale (str. pyramidale: 42.8 \pm 1.4% of CRH-ir

cells; str. radiatum: 4.6 \pm 2.1% of CRH-ir cells; Fig. 3a; Table 2). In contrast, CCK was preferentially co-expressed in CRH interneurons residing in str. radiatum (str. pyramidale: 16.4 \pm 1.6% of CRH-ir cells; str. radiatum: 33.9 \pm 1.8% of CRH-ir cells; Fig. 3b; Table 2). The pattern of CR co-expression with CRH was still different: 20–25% of CRH-expressing neurons also expressed the protein (str. pyramidale: 25.8 \pm 1.2% of CRH-ir cells; str. radiatum: 21.0 \pm 1.5% of CRH-ir cells. Figure 3c; Table 2). No co-localization was detected between CRH and SOM or CRH and CB (Fig. 3d, e; Table 2).

Electrophysiological properties of CRH interneurons in the pyramidal cell layer and str. radiatum of area CA1

Having confirmed the tdTomato-Crh mouse line as a valuable research tool, we conducted whole-cell current-clamp recordings from CRH interneurons located within the pyramidal cell layer and str. radiatum of area CA1. Experiments determined the action potential firing in response to a current stimulus protocol (see “Materials and methods”)

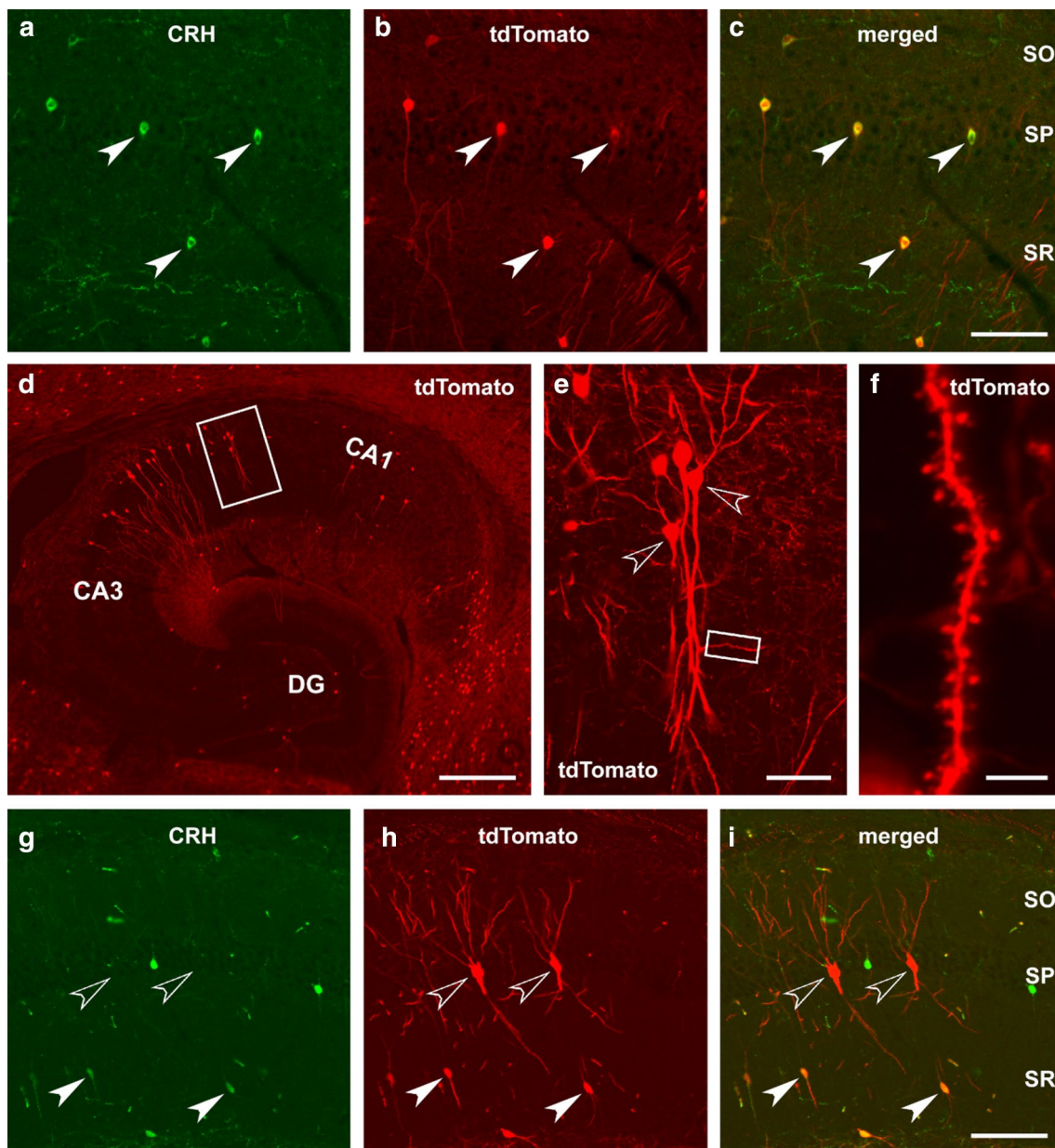


Fig. 2 Colocalization of CRH and tdTomato-reporter in the hippocampus of *Crh-IRES-Cre;Ai14* tdTomato mouse. **a–c** tdTomato reporter-expressing neurons with a shape of interneuron (red) co-expressed (arrowheads) CRH (green) in strata pyramidale (SP) and radiatum (SR) of area CA1. **d–f** A subset of tdTomato-expressing cells with typical morphology of pyramidal cells was primarily observed in the transitional area between CA1 and CA3. Framed area in **d** was magnified in **f** to show the pyramidal-like reporter-express-

ing cells (empty arrowheads). A dendritic branch (boxed in **e**) was further magnified in **i**, and numerous dendritic spines were observed on the branch. **g–i** Reporter-expressing cells with a shape of pyramidal cell (empty arrowhead) located in the stratum pyramidale. These cells did not express CRH. In the same section, those interneuron-like reporter-expressing cells located in the stratum radiatum co-expressed CRH (arrowheads). Scale bars 125 μm (**a–c**, **g–i**), 380 μm (**d**), 50 μm (**e**), and 4 μm (**f**)

and characterized the intrinsic neuronal and action potential properties.

Pyramidal cell layer

The action potential firing pattern in response to a 100 pA current injection could be divided into two broad groups:

type 1 that displayed fast adaptation (FA) and type 2 that did not (Fig. 4a). The majority of CRH interneurons were type 1 (11 out of 17 cells) and had a mean spike frequency of 22.3 ± 3 Hz in response to 100 pA injected current ($n = 11$, Fig. 4b). Type 2 CRH interneurons were significantly more excitable, having a mean action potential frequency of 46.7 ± 6 Hz in response to the same current

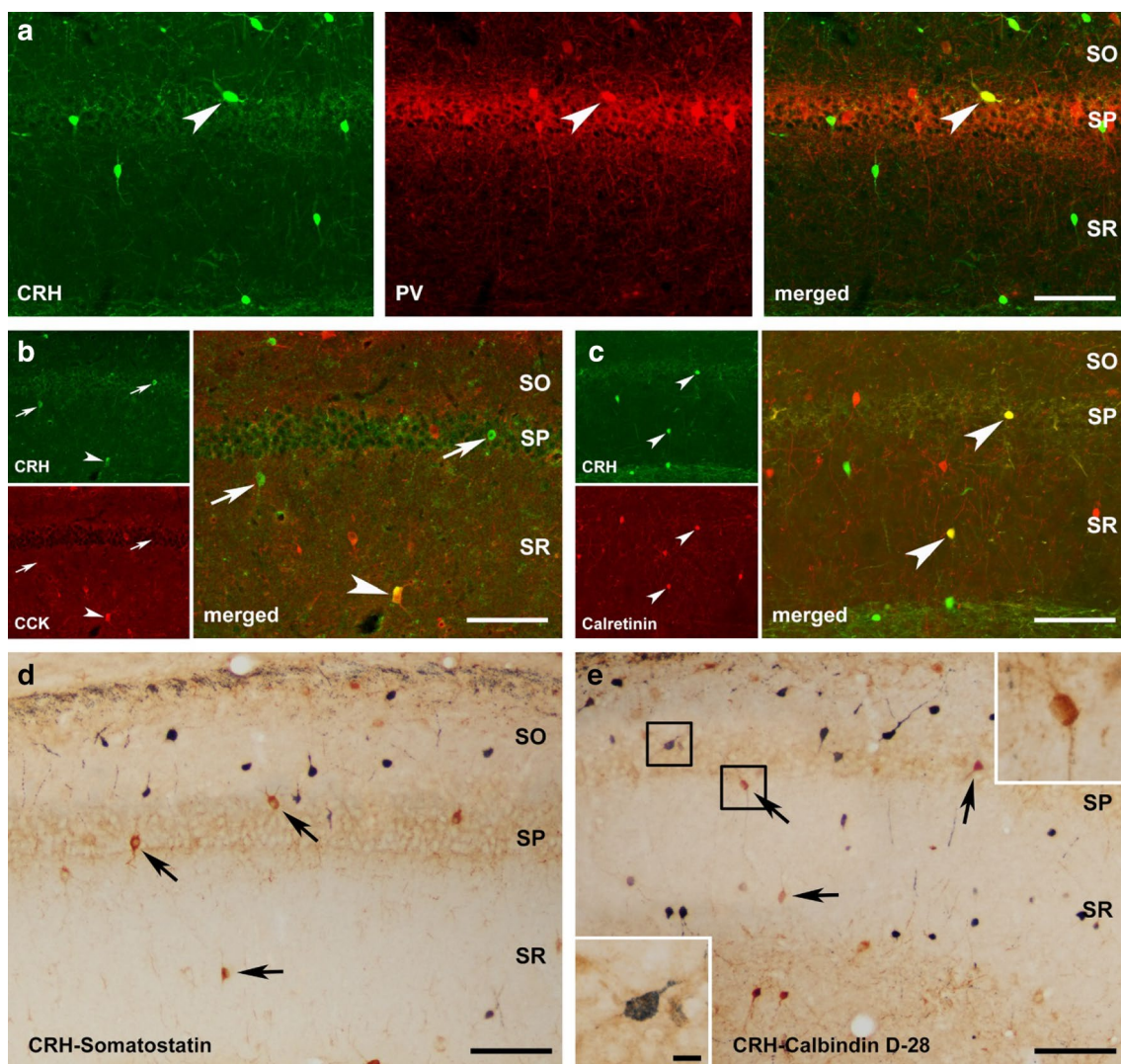


Fig. 3 The co-localization of CRH-ir interneurons and interneuron markers in CA1 stratum pyramidale and radiatum of adult C57BL/6J mice. **a** A subgroup of CRH-ir cells in the str. pyramidale co-expressed parvalbumin (PV; arrowhead), but those in the radiatum seldom co-expressed this calcium-binding protein. **b** Co-localization was detected between CRH and cholecystikinin (CCK) in str. pyramidale and radiatum. CCK cells were more concentrated in the radiatum but were also found in the pyramidale. An example cell in the radiatum co-expressed CRH and CCK (arrowhead). Arrows denote CRH single-labeled cells. **c** A group of CRH-ir neurons in str. pyramidale and radiatum co-expressed calretinin (red). Calretinin-ir

cells were distributed in the radiatum rather than in the pyramidale. **d** Somatostatin-expressing cells (dark-blue) were primarily detected in the stratum oriens (SO) in area CA1, but less found in the pyramidale and radiatum. No co-localization was found between CRH (brown, arrows) and somatostatin. **e** Co-localization of CRH (brown, arrows) and calbindin D-28 (dark-blue) was not detected in area CA1. Calbindin D-28 was expressed in one population of interneurons as shown here (a group of pyramidal cells also expressed calbindin D-28, not shown). SO, stratum oriens; SP, stratum pyramidale; SR, stratum radiatum. Scale bars 125 μm (**a–c**), 120 μm (**d**), 130 μm (**e**), and 15 μm (inset in **e**)

injection ($n=6$, Fig. 4a). Consistent with this observation, the *I–O* curve of type 2 CRH interneurons showed a significant leftward shift of type 1 neurons (Fig. 4b). Interestingly, type 2 CRH interneurons could be subdivided into two populations based upon their firing frequency and the relative degree of slow adaptation of action potential firing (Fig. 4a). Slow adapting (SA) type 2 neurons (Type 2a) had a mean spike frequency of 34.8 ± 3 Hz ($n=4$) in response to 100 pA current step, while fast-spiking

(FS)-like cells (type 2b) were much less common having a mean frequency of 70.3 Hz ($n=2$, Fig. 4a). Although we specifically did not target the CRH-negative pyramidal-like cells (i.e., Fig. 2d, e), all recorded cells were filled with neurobiotin and processed for CRH expression post hoc (Fig. 4c). For comparison, we next recorded the firing properties of CA1 pyramidal cells, which had a mean spike frequency in response to a 100 pA current injection of 22.7 ± 4 Hz ($n=7$, Fig. 4a). Pyramidal cells were

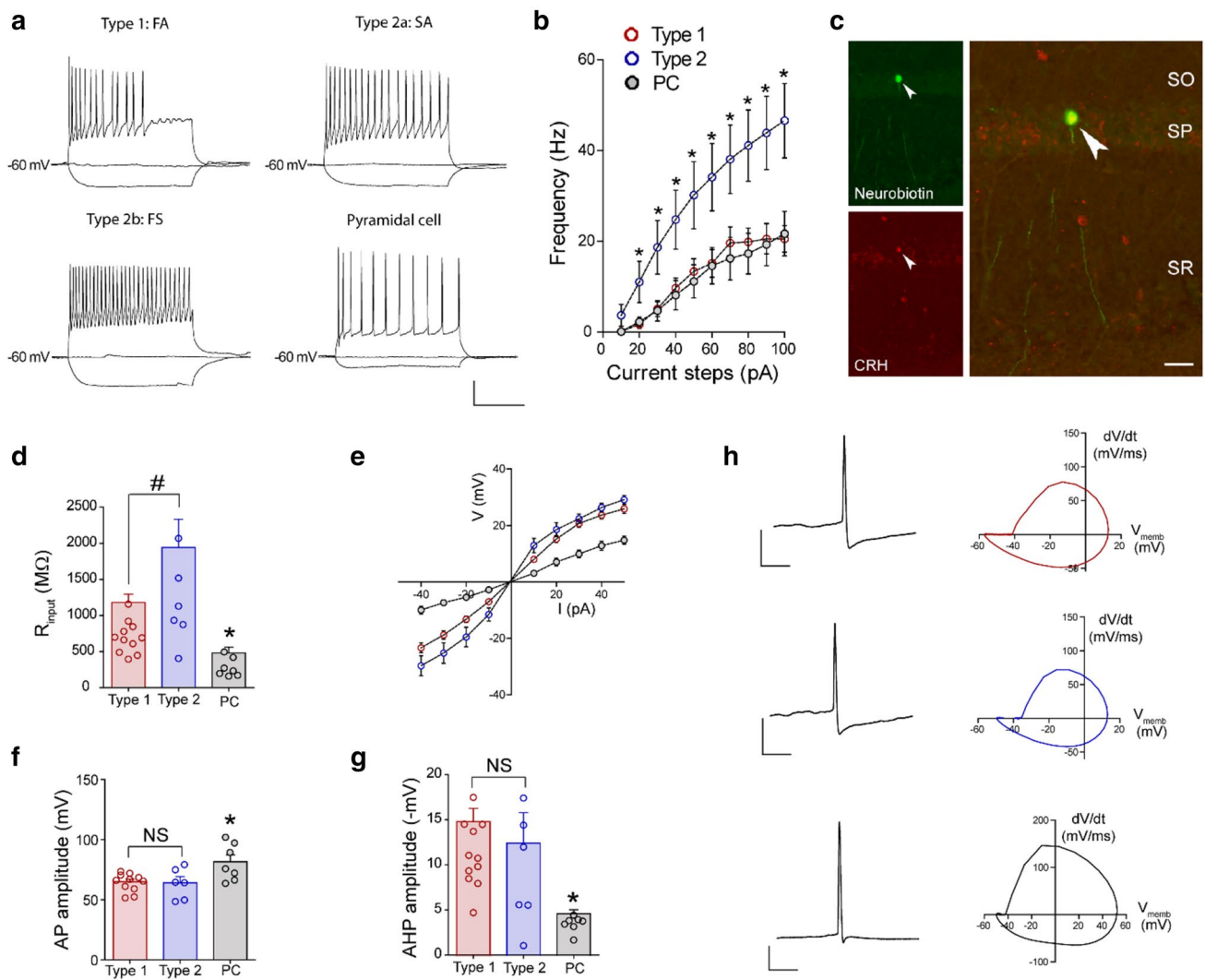


Fig. 4 CRH interneurons located in the str. pyramidale have heterogeneous firing properties and homogeneous action potential properties. **a** Type 1 CRH interneurons display rapid spike frequency adaptation in response to a depolarizing current injection (100 pA), while type 2 neurons showed significantly less adaptation. The degree of spike frequency adaptation varied across type 2 neurons, with type 2a and type 2b neurons exhibiting slow adaptation (SA) and fast spiking (FS), respectively. Note that all subtypes differed from pyramidal cells. **b** Graph summarizing the mean spike frequency associated with depolarizing current steps for type 1 ($n=11$) and type 2 ($n=6$) CRH interneurons and pyramidal cells ($n=7$). Note that type 2 CRH interneurons had a significantly higher mean spike frequency compared to type 1 and pyramidal cells ($*p < 0.05$ unpaired Student's *t* vs pyramidal cell and type 1 neurons). **c** Confirmation of neurochemical profile of recorded neuron. Representative image of a single neuron recorded from the CA1 pyramidal cell layer showing immunoreactivity for neurobiotin (green) and CRH (red). **d** Bar graph illustrating the mean input resistance (R_{input}) measured for type 1 and type 2 CRH interneurons and CA1 pyramidal cells. Note that both type

1 and type 2 CRH interneurons have a significantly higher R_{input} of pyramidal cell ($p < 0.05$ unpaired Student's *t* test), while type 2 CRH interneurons have a significantly greater R_{input} than their type 1 counterparts. **e** Graph illustrating the I - V relationship for each type of neuron. Note that pyramidal cells display a near linear relationship, while both types of CRH interneurons do not. Bar graphs illustrating the mean action potential (**f**) and afterhyperpolarization (AHP; **g**) amplitudes recorded from type 1 ($n=11$) and type 2 ($n=6$) CRH interneurons and pyramidal cells ($n=7$). Note that there was no significant difference between type 1 and type 2 CRH interneurons ($p > 0.05$ unpaired Student's *t* test), while pyramidal cells had a significantly larger action potential amplitude and smaller AHP of CRH interneurons ($p < 0.05$ unpaired Student's *t* test). **h** Exemplar representative action potentials (left), and accompanying phase plane plots (right), recorded from a type 1 (top), a type 2 (middle) CRH interneuron and a CA1 pyramidal cell (bottom). Note the smaller peak amplitude and larger AHP of action potentials recorded from CRH interneurons. Scale bars $y=20$ mV and $x=20$ ms in **a, h**; $60 \mu\text{m}$ in **c**

significantly less excitable than the type 2 CRH interneurons, while no significant difference was observed with type 1 cells (Fig. 4b). Both CRH interneuron populations

had a significantly higher R_{input} than pyramidal cells (Fig. 4d; Table 3a); in addition, the R_{input} of type 2 CRH interneurons was significantly greater than that of their

Table 3 Properties of CRH interneurons recorded from stratum pyramidale and stratum radiatum of the hippocampus CA1

(a). Stratum pyramidale	Type 1 (<i>n</i> = 11)	Type 2 (<i>n</i> = 6)	Pyramidal cells (<i>n</i> = 7)
V_{Membrane} (mV)	-61.2 ± 1.7	-63.1 ± 3.7	-67.9 ± 3.1
R_{input} (M Ω)	$670 \pm 67^*$	$879 \pm 110^{*\dagger}$	294 ± 39
τ_{membrane} (ms)	39.2 ± 5.2	40.3 ± 2.7	38.2 ± 3.2
Threshold (mV)	$-50.8 \pm 0.8^*$	$-51.7 \pm 0.9^*$	-57.4 ± 1.2
Rheobase (pA)	46.4 ± 7.2	$21.7 \pm 4.8^{*\dagger}$	47.1 ± 8.1
Latency to 1st spike (ms)	$8.7 \pm 1.0^*$	$9.9 \pm 3.5^*$	34.1 ± 9.6
Amplitude (mV)	$64.3 \pm 2.3^*$	$63.5 \pm 5.1^*$	80.9 ± 5.8
Half-width (ms)	1.7 ± 0.1	2.0 ± 0.1	1.9 ± 0.1
Rise time (ms)	1.0 ± 0.1	1.2 ± 0.2	0.9 ± 0.1
Decay time (ms)	1.3 ± 0.1	1.6 ± 0.2	1.5 ± 0.1
AHP amplitude (mV)	$-11.1 \pm 1.1^*$	$-9.3 \pm 3.1^*$	-3.5 ± 0.3
(b) Stratum radiatum	Type 1 (<i>n</i> = 3)	Type 2 (<i>n</i> = 6)	
V_{membrane} (mV)	-69.2 ± 0.8	-66.2 ± 2.9	
R_{input} (M Ω)	$746 \pm 75^*$	$802 \pm 82^*$	
τ_{membrane} (ms)	37.3 ± 2.7	38.8 ± 2.1	
Threshold (mV)	-51.3 ± 0.8	-50.5 ± 1.9	
Rheobase (pA)	33.3 ± 6.7	26.7 ± 6.2	
Latency to 1st spike (ms)	8.4 ± 2.1	$10.1 \pm 2.3^*$	
Amplitude (mV)	$48.2 \pm 1.9^*$	$58.6 \pm 3.3^*$	
Half-width (ms)	1.9 ± 0.1	1.5 ± 0.3	
Rise time (ms)	1.2 ± 0.1	1.5 ± 0.3	
Decay time (ms)	1.5 ± 0.2	1.4 ± 0.2	
AHP amplitude (mV)	$-8.1 \pm 2.9^*$	$-11.4 \pm 2.0^*$	

**p* < 0.05 vs pyramidal cell, unpaired Student's *t* test†*p* < 0.05 vs type 1

type 1 counterparts (Fig. 4d; Table 3a). The latency to first spike, in response to 100 pA injected current was significantly shorter for both types of CRH interneurons compared with pyramidal cells (Table 2a). Pyramidal cells exhibited a linear *I*–*V* relationship (Fig. 4e), while in both types of CRH interneurons a non-linear relationship was observed (Fig. 4e).

Spontaneous action potential firing was observed in ~67% (11 out of 17 cells) and ~60% (4 out of 7 cells) of CRH interneurons and pyramidal cells, respectively. No significant difference was observed between the mean membrane potential recorded from pyramidal cells or CRH interneurons (Table 3a) or the membrane time constant (τ_{membrane} ; Table 3a). Typically, a lack of spontaneous firing was observed in neurons (both pyramidal cells and interneurons) that had a more hyperpolarized membrane potential. The amplitude of action potentials recorded from CRH interneurons (both type 1 and type 2) was significantly reduced compared to pyramidal cells, while the AHP was significantly greater (Fig. 4f–h; Table 3a). No differences were observed in the action potential half-width, rise time or deactivation kinetics (Table 3a).

Stratum radiatum

We next adopted a similar approach to characterize the properties of CRH-expressing interneurons located within the stratum radiatum of area CA1. As in the pyramidal cell layer, the action potential firing patterns recorded from radiatum CRH interneurons could be divided into two broad groups: type 1 neurons that displayed fast adaptation (FA) and type 2 neurons that did not (Fig. 5a). The majority of CRH interneurons recorded from the radiatum were type 2, exhibiting slow or minimal adaptation of action potential firing (5 out of 8 cells). Type 2 neurons were significantly more excitable than fast-adapting type 1 neurons (Fig. 5b). All neurons were labeled with neurobiotin and analyzed post hoc (Fig. 5c). No significant differences in the R_{input} , latency to first spike or the *I*–*V* relationship were observed between type 1 and type 2 CRH interneurons in the radiatum (Fig. 5d, e; Table 3b).

Spontaneous action potential firing was observed in 3 out of 9 CRH interneurons recorded in the stratum radiatum, with type 1 neurons having no spontaneous activity. The mean membrane potential and τ_{membrane} of type 1 and type 2 CRH interneurons were not significantly different

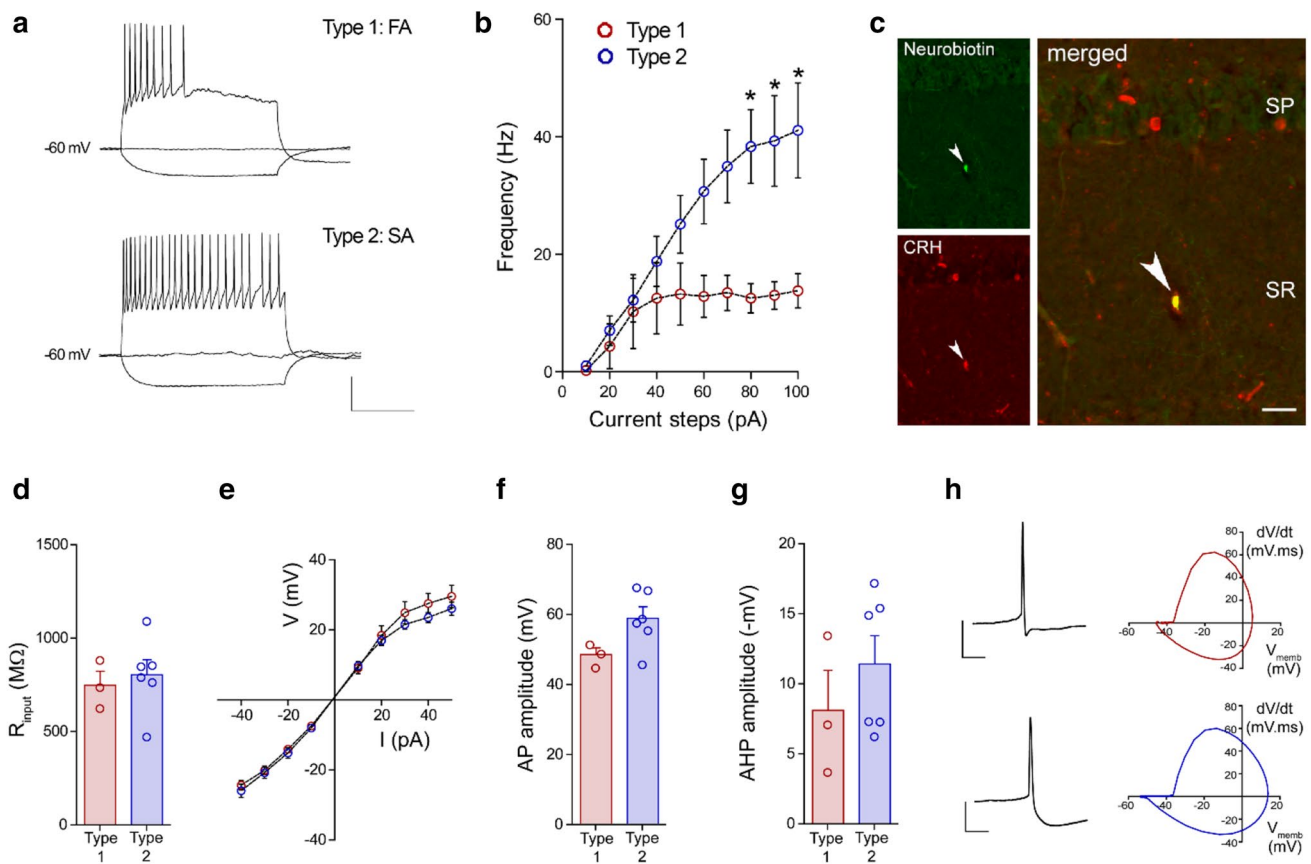


Fig. 5 CRH interneurons located in the str. radiatum have heterogeneous firing patterns, but similar action potential and intrinsic properties. **a** Type 1 CRH interneurons display rapid spike frequency adaption (FA) in response to a depolarizing current injection (100 pA), while type 2 neurons showed significantly less adaptation (SA). **b** Graph summarizing the mean spike frequency associated with depolarizing current steps for type 1 ($n=3$) and type 2 ($n=6$) CRH interneurons. Note that type 2 CRH interneurons had a significantly higher mean spike frequency compared to type 1 ($*p < 0.05$ unpaired Student's t test vs type 1 neuron). **c** Confirmation of neurochemical profile of recorded neuron. Representative image of a single neuron recorded from the CA1 str. radiatum showing immunoreactivity for

neurobiotin (green) and CRH (red). **d** Bar graph illustrating the mean input resistance (R_{input}) measured for type 1 and type 2 CRH interneurons. **e** Graph illustrating the I - V relationship for each type of CRH interneuron. Note that there is no difference in the I - V relationship. Bar graphs illustrating the mean action potential (**f**) and afterhyperpolarization (AHP; **g**) amplitudes recorded from type 1 ($n=3$) and type 2 ($n=6$) CRH interneurons. Note that there was no significant difference between type 1 and type 2 CRH interneurons ($p > 0.05$ unpaired Student's t test). **h** Exemplar representative action potentials (left), and accompanying phase plane plots (right), recorded from a type 1 (top) and a type 2 (bottom) CRH interneuron. Scale bars $y=20$ mV and $x=20$ ms in **a**, **h**; $60 \mu\text{m}$ in **c**

(Table 3b). Furthermore, no significant differences were observed in any of the properties of action potentials recorded from type 1 and type 2 CRH interneurons recorded in this layer (Fig. 4f–h; Table 3b).

Discussion

Here we provide the first functional/electrophysiological, neurochemical and neuroanatomical evidence that CRH-expressing interneurons located in str. pyramidale and str. radiatum of field CA1 are a heterogeneous population that cannot be classified into one distinct subtype using conventional criteria. These findings raise the possibility that CRH

interneuron subtypes may have functionally distinct roles in the diverse processes executed within hippocampal circuitry.

Neurochemical and electrophysiological phenotype of CRH-interneurons

Our in situ hybridization and immunocytochemistry data are consistent with a number of previous studies using mice and rats, which demonstrated that CRH and GAD are co-expressed (Yan et al. 1998a, b; Chen et al. 2001, 2004, 2015; Hooper and Maguire 2016). Additionally, using a dual-labeling approach we found a pattern of CRH co-localization, or indeed lack of, with different Ca^{2+} -binding proteins (e.g., PV, CR, CB) and other peptides (CCK, SOM) that was largely consistent with previous reports in both rats and mice

(Yan et al. 1998b; Chen et al. 2012, 2015). Interestingly, whereas the expression of CCK was previously reported not to overlap with that of CRH in rats (Chen et al. 2012), this seems to differ in mice, with CCK–CRH co-localization in neurons located in both str. pyramidale and str. radiatum. This finding suggests potential species differences may exist and should be a consideration for future studies. In this regard, it should be noted that CRH co-localization has only been investigated, in both mice and rats, using a relatively small proportion of known interneuron markers, and additional experiments are required to further characterize these neurons (see section below). While our findings at the neurochemical level are generally in agreement with the literature, they are largely in contrast to a recent study that characterized the properties of CRH interneurons in CA1 (Hooper and Maguire 2016). Such a discrepancy may be related to the use of different *Crh*-Cre driver (i.e., *Crh-IRE5-Cre* and *Crh-GFP*) and/or reporter mouse lines (i.e., Ai14, Ai9), which has recently been suggested to result in the selective labeling of different subpopulations of CRH interneurons (Hooper et al. 2018). Indeed, the fidelity of different *Crh* transgenic mouse lines has been the focus of recent attention (Martin et al. 2010; Chen et al. 2015; Hooper and Maguire 2016; Kono et al. 2017; Peng et al. 2017; Walker et al. 2018). In our hands, dual immunocytochemistry showed a high level of congruence between the reporter expression (i.e., tdTomato) and native CRH in the *Crh-IRE5-Cre* mouse (present study; Chen et al. 2015), although, consistent with others we did observe non-specific reporter labeling within the dentate gyrus (Walker et al. 2018), as well as a population of pyramidal-like neurons on the CA1/2 border (Fig. 2d–f). Importantly, the pattern of reporter expression and the anatomical features of labeled neurons were largely consistent with previous studies characterizing the distribution of CRH within the hippocampus (Yan et al. 1998a, b; Chen et al. 2001). While selective labeling of different populations of CRH-expressing interneurons may account for some of the observed differences in neurochemical and physiological (below) phenotypes with previous studies (Hooper and Maguire 2016), it remains to be determined whether the expression pattern of the native peptide differs between mouse lines. Certainly, differences in the immunocytochemical methods, such as the duration and concentration of CRH antibody used cannot be ruled out as potential causes for the reported differences, while ascertaining whether expression of the peptide is dynamic (i.e., not static), changing in response to specific physiological states may also be important for explaining the observed differences.

The heterogeneity of CRH interneurons was similarly apparent at the electrophysiological level. CRH interneurons located in both hippocampal layers were classified based upon the degree of spike frequency adaptation displayed,

with fast and non-fast adapting groups (Figs. 4, 5). Many factors, including Na⁺-channel inactivation, M-type K⁺ currents, Ca²⁺-dependent K⁺ channels and Ca²⁺-activated Cl⁻ channels have been suggested to influence spike frequency adaptation (Brown and Adams 1980; Madison and Nicoll 1984; Fleidervish et al. 1996; Stocker 2004) and further studies are required to determine whether these may be important in differentially regulating the excitability of CRH interneuron subtypes. While differences in spike frequency adaptation were observed in the two groups of CRH interneurons, many of the intrinsic properties and action potential characteristics were the same. A notable exception was a higher R_{input} of type 2 neurons located in the pyramidal cell layer. This higher R_{input} likely contributes to the increased excitability of these cells as illustrated by the lower rheobase and increased spike frequency of these cells. Additionally, CRH interneurons (both type 1 and type 2) had firing characteristics, intrinsic properties (e.g., R_{input} , threshold, latency to spike) and action potential properties (e.g., peak, AHP amplitude) that were significantly different from CA1 pyramidal cell.

Notably, the electrophysiological properties reported here are only partially consistent with the findings from a recent study (Hooper and Maguire 2016). As mentioned above, the apparent discrepancy between studies may be due to the use of different *Crh*-Cre driver (*Crh-IRE5-Cre* and *Crh-GFP*) and/or reporter mouse lines (Ai14 and Ai9) and the possible selective labeling of different subpopulations of CRH neurons associated with these transgenic animals.

What class of interneurons do CRH-expressing cells represent?

Hippocampal interneurons are highly diverse, comprising over 20 distinct subtypes (Klausberger and Somogyi 2008). Our data suggests that CRH interneurons located in CA1 str. pyramidale and str. radiatum cannot be classified as a single subtype based upon conventional anatomical, neurochemical and electrophysiological criteria. Rather, it would appear that CRH may be co-expressed in subpopulations of previously described interneuron subtypes (Fig. 3) (Freund and Buzsaki 1996; Yan et al. 1998b; Klausberger and Somogyi 2008).

Within the pyramidal cell layer, a significant proportion of CRH interneurons co-expressed the Ca²⁺-binding protein PV (~43% of cells in CA1; Table 2), a neurochemical marker associated with fast-spiking basket cells, axo-axonic and bistratified cells (Freund and Buzsaki 1996) (Fig. 6). This observation is consistent with electron microscopy demonstrations of the co-expression of CRH and PV in a subpopulation of axo-axonic and basket cells in the pyramidal cell layer (Yan et al. 1998b). Functionally, PV-expressing interneurons are typically associated with a fast-spiking

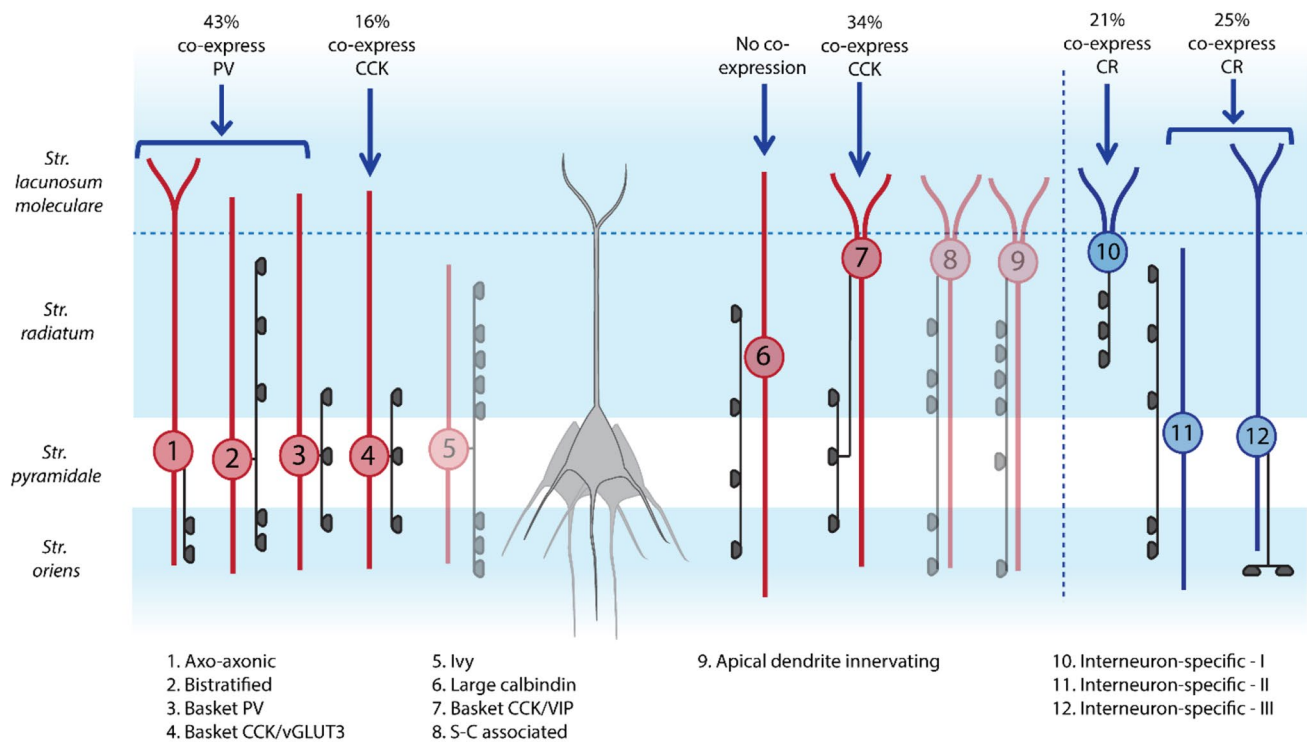


Fig. 6 Schematic illustration summarizing potential CRH co-expression within conventional interneuron subtypes located within str. pyramidale and str. radiatum of the hippocampus CA1. Schematic illustrating the nature of the dendritic ramifications for each interneuron subtype along with the respective subcellular domain(s) that they innervate on CA1 pyramidal cells (grey) and in some cases interneurons. Of those interneuron subtypes that have their soma located in str. pyramidale, the majority of CRH-expressing interneurons co-express PV (43%; 1–3), while a smaller population of cells co-expressed CCK (16%; 4). CRH co-expression has not been explored in Ivy cells (5; faded). Note that these cells share similar electro-

physiological properties to CRH-expressing interneurons. Within str. radiatum CRH was only found to co-express CCK (34%; 6), with no co-localization with calbindin (7). The expression of CRH in S–C associated (8; faded) and apical dendrite innervating (9; faded) interneurons has not been determined. Note that CR is co-expressed in 21% and 25% of CRH interneurons located in str. radiatum (10) and str. pyramidale (11,12), respectively, raising the possibility that the neuropeptide may be expressed in a population of interneuron-specific interneurons. Note that our data indicates that CRH may be expressed in subpopulations of at least four subtypes of interneuron

phenotype (i.e., > 50 Hz at 22 °C; > 150 Hz at 35 °C) and rapidly decaying action potentials (Hu et al. 2014). Our electrophysiological data indicate that only a small proportion of CRH interneurons within CA1 pyramidal cell layer were fast-spiking (2 out of 17 cells), and all had a broad action potential half-width (Table 3). Whereas our anatomical data would suggest a higher fraction of fast-spiking CRH interneurons, it is important to realize that all three classes of described PV-expressing interneurons exhibit a variety of firing patterns in response to depolarizing current pulses (i.e., heterogeneous spike frequency adaptation) (Buhl et al. 1994, 1996; Pawelzik et al. 2002). Such functional heterogeneity may be associated with the co-expression of other peptides, e.g., SST and NPY in bistratified interneurons (Pelkey et al. 2017) although further studies are required to confirm this notion. Thus, it is tempting to speculate that CRH co-expression may be associated with different firing patterns of these PV-containing interneuron classes, either through different expression profile of specific voltage-gated

ion channels (e.g., K^+ channels) or via the peptide modulating intrinsic neuronal excitability in an autocrine manner. In pyramidal cells, CRH activation of CRHR1 results in an increase in neuronal excitability at least in part through the inhibition of Ca^{2+} -dependent K^+ channel function (Aldenhoff et al. 1983; Gunn et al. 2017), as well as through the attenuation of fast A-type and delayed rectifier K-type K^+ currents (Kratzer et al. 2013). Given that such an increase in the excitability of CRH interneurons is not apparent here, and to date, CRH receptors have only been identified on pyramidal cells, it would seem more likely that CRH co-expression may be associated with changes in the expression of ion channels that underlie intrinsic neuronal properties.

Unexpectedly (Chen et al. 2012), CCK co-expression with CRH was observed in a significant number of interneurons residing in str. radiatum, and to a lesser extent those located in str. pyramidale. Similar to PV-expressing interneurons, those expressing CCK typically innervate the perisomatic domains of pyramidal cells (Freund and Buzsaki 1996),

although they predominantly exhibit a regular firing pattern more reminiscent of that observed in type 2 neurons located in both laminae (Pawelzik et al. 2002). These data support our prior reports of perisomatic CRH-containing axon terminals and boutons, studies carried out at both light microscopy and electron microscopy levels (Chen et al. 2004).

A smaller population of CRH-interneurons in str. pyramidale and radiatum co-expressed CR, a peptide that has been associated with diverse interneuron subtypes (Fig. 6) (Freund and Buzsaki 1996; Gulyas et al. 1996; Tricoire et al. 2011). Future anatomical analysis of their dendrites (e.g., spiny vs non-spiny) and their axonal ramifications would provide useful information regarding their target neurons (pyramidal cell or interneuron) and hence potential functional role(s). The relatively slow firing rate (i.e., < 50 Hz) and broad action potential half-width (i.e., indistinguishable from pyramidal cell) observed in the majority of CRH interneurons in str. pyramidale is reminiscent of Ivy cells, which typically express neuronal nitric oxide synthase (nNOS) and NPY (Fuentelba et al. 2008). Given that both NPY and CRH-expressing interneurons have a broad action potential it is tempting to speculate that this is a characteristic required for the mobilization and release of small dense core vesicles containing the neuropeptide. A more extensive characterization of the neurochemical markers (e.g., nNOS, VIP and NPY) and the anatomy of CRH interneurons would prove useful in further classifying this population of neurons. Indeed, elucidating the nature of the dendritic and axonal projections of the diverse subpopulations of CRH interneurons in both hippocampal laminae would provide fundamental information regarding the likely origin of afferent inputs to these neurons as well as the subcellular regions that they innervate on their target cells. Such information may provide clues as to the possible role(s) of these cells in hippocampal function (see below).

Are CRH-expressing neurons more diverse than other populations of neuropeptide-defined cells?

Whether the level of neurochemical, anatomical and electrophysiological heterogeneity observed amongst CRH interneurons located in hippocampus CA1 is a unique feature to this class of cells is an interesting proposition. Indeed, when considered collectively our neurochemical and electrophysiological data suggest that at least four subtypes of CRH interneurons are expressed across strata pyramidale and radiatum. Such heterogeneity appears to be greater than the vast majority of other interneuron subtypes. For example, PV-ir neurons were primarily fast spiking, while the majority of CCK expressing neurons were regular spiking (Pawelzik et al. 2002). This raises the possibility that the described heterogeneity is actually associated with the expression of

CRH. The recent observation that CRH expressing interneurons within the extended and central nucleus of the amygdala exhibit neurochemical and structural heterogeneity (e.g., spiny and aspiny cells) lends support to this notion (Dedic et al. 2018).

Functional implications of CRH interneuron heterogeneity

The apparent heterogeneity of CRH-expressing interneurons at neurochemical, localization and electrophysiological domains raises the possibility that different types of CRH-expressing interneurons may perform specific functions within the hippocampus. Here, one has to consider also the distinct and potentially opposing effects of CRH release vs GABA release from these cells.

The excitatory effects of CRH upon pyramidal cell function have been well documented [for recent review see (Gunn and Baram 2017)]. These actions are mediated primarily via CRHR1 (Refojo et al. 2011; Kratzer et al. 2013; Gunn et al. 2017), located at distinct somatic and dendritic sites on these cells (Chen et al. 2000, 2010, 2012). Currently, the neuropeptide is believed to diffuse from its release site at inhibitory synapses, via volume transmission, and activate CRHR1 receptors located at adjacent excitatory synapses (Chen et al. 2012; van den Pol 2012). While it remains to be determined whether CRH receptors are expressed on specific interneuron subtypes, the ability of the neuropeptide to modulate interneuron activity would be a potentially powerful mechanism by which hippocampal network activity could be regulated.

In addition to the postsynaptic actions of CRH, our understanding of how this peptide is released from these interneurons is extremely limited. Classically, neuropeptide release from dense core vesicles in the hypothalamus occurs from dendrites and is thought to require high-frequency excitatory drive (van den Pol 2012). Within the hippocampus, there is no evidence to suggest that CRH is released from dendritic sites, rather the peptide congregates in the axon terminal where it is presumably released (Yan et al. 1998b; Chen et al. 2004, 2012). Whether CRH release is dependent upon specific frequencies of input that may occur during certain physiological or pathological contexts is unclear. In this regard, stress is known to trigger CRH release within the hippocampus (Chen et al. 2004) and this peptide has been implicated in mediating a number of stress-related effects upon hippocampal function (Chen et al. 2010, 2016). Furthermore, it is important to consider that the expression of CRH within the hippocampus may not be static rather it is conceivable that levels are dynamically regulated in response to specific physiological and/or pathological events such as stress. The neuropeptide is stably expressed within hippocampal interneurons throughout development, i.e.,

independent of stress (Chen et al. 2001), while exposure to adverse early life experience increases the number of CRH-expressing interneurons in field CA1 and CA3 (Ivy et al. 2010). However, the effect that acute stressor exposure has upon CRH expression, and the potential functional implications, remain to be determined.

The development of Crh reporter mouse lines has provided a useful tool to investigate the functional significance of these cells during stress exposure and recent studies have begun to utilize optogenetic and chemogenetic (DREADDs) approaches to investigate the functional role(s) that these neurons play during stressor exposure (Hooper et al. 2018). However, interpreting findings from such experiments will likely be complicated by the described heterogeneity of CRH interneurons, as well as the non-specific reporter labeling and the substantial differences in the fidelity of the different Crh reporter mouse lines (Chen et al. 2015; Hooper and Maguire 2016; Walker et al. 2018).

In summary, hippocampal CRH-expressing interneurons are an especially diverse and heterogeneous group of cells. It is tempting to speculate that the crucial importance of stress-induced changes in learning and memory might be at play: executing a rapid and complex spatiotemporal set of programs to respond, remember and adapt to stress signals should require a highly diverse and potent set of neurons within the hippocampal formation.

Funding National Institutes of Health, NS28912, MH096889, MH73136.

Compliance with ethical standards

Conflict of interest Authors declare no conflict of interest.

References

- Aldenhoff JB, Gruol DL, Rivier J, Vale W, Siggins GR (1983) Corticotropin releasing factor decreases postburst hyperpolarizations and excites hippocampal neurons. *Science* 221:875–877
- Bartos M, Vida I, Jonas P (2007) Synaptic mechanisms of synchronized gamma oscillations in inhibitory interneuron networks. *Nat Rev Neurosci* 8:45–56
- Brown DA, Adams PR (1980) Muscarinic suppression of a novel voltage-sensitive K⁺ current in a vertebrate neurone. *Nature* 283:673–676
- Buhl EH, Han ZS, Lorinczi Z, Stezhka VV, Karnup SV, Somogyi P (1994) Physiological properties of anatomically identified axo-axonic cells in the rat hippocampus. *J Neurophysiol* 71:1289–1307
- Buhl EH, Szilagy T, Halasy K, Somogyi P (1996) Physiological properties of anatomically identified basket and bistratified cells in the CA1 area of the rat hippocampus in vitro. *Hippocampus* 6:294–305
- Chen Y, Brunson KL, Muller MB, Cariaga W, Baram TZ (2000) Immunocytochemical distribution of corticotropin-releasing hormone receptor type-1 (CRF(1))-like immunoreactivity in the mouse brain: light microscopy analysis using an antibody directed against the C-terminus. *J Comp Neurol* 420:305–323
- Chen Y, Bender RA, Frotscher M, Baram TZ (2001) Novel and transient populations of corticotropin-releasing hormone-expressing neurons in developing hippocampus suggest unique functional roles: a quantitative spatiotemporal analysis. *J Neurosci* 21:7171–7181
- Chen Y, Brunson KL, Adelmann G, Bender RA, Frotscher M, Baram TZ (2004) Hippocampal corticotropin releasing hormone: pre- and postsynaptic location and release by stress. *Neuroscience* 126:533–540
- Chen Y, Rex CS, Rice CJ, Dube CM, Gall CM, Lynch G, Baram TZ (2010) Correlated memory defects and hippocampal dendritic spine loss after acute stress involve corticotropin-releasing hormone signaling. *Proc Natl Acad Sci USA* 107:13123–13128
- Chen Y, Andres AL, Frotscher M, Baram TZ (2012) Tuning synaptic transmission in the hippocampus by stress: the CRH system. *Front Cell Neurosci* 6:13
- Chen Y, Molet J, Gunn BG, Ressler K, Baram TZ (2015) Diversity of reporter expression patterns in transgenic mouse lines targeting corticotropin-releasing hormone-expressing neurons. *Endocrinology* 156:4769–4780
- Chen Y, Molet J, Lauterborn JC, Trieu BH, Bolton JL, Patterson KP, Gall CM, Lynch G, Baram TZ (2016) Converging, synergistic actions of multiple stress hormones mediate enduring memory impairments after acute simultaneous stresses. *J Neurosci* 36:11295–11307
- Cobb SR, Buhl EH, Halasy K, Paulsen O, Somogyi P (1995) Synchronization of neuronal activity in hippocampus by individual GABAergic interneurons. *Nature* 378:75–78
- Colgin LL (2016) Rhythms of the hippocampal network. *Nat Rev Neurosci* 17:239–249
- Cossart R, Petanjek Z, Dumitriu D, Hirsch JC, Ben-Ari Y, Esclapez M, Bernard C (2006) Interneurons targeting similar layers receive synaptic inputs with similar kinetics. *Hippocampus* 16:408–420
- Dedic N, Kuhne C, Jakovcevski M, Hartmann J, Genewsky AJ, Gomes KS, Anderzhanova E, Pohlmann ML, Chang S, Kolarz A, Vogl AM, Dine J, Metzger MW, Schmid B, Almada RC, Ressler KJ, Wotjak CT, Grinevich V, Chen A, Schmidt MV, Wurst W, Refojo D, Deussing JM (2018) Chronic CRH depletion from GABAergic, long-range projection neurons in the extended amygdala reduces dopamine release and increases anxiety. *Nat Neurosci* 21:803–807
- Farrant M, Nusser Z (2005) Variations on an inhibitory theme: phasic and tonic activation of GABA(A) receptors. *Nat Rev Neurosci* 6:215–229
- Fleiderovich IA, Friedman A, Gutnick MJ (1996) Slow inactivation of Na⁺ current and slow cumulative spike adaptation in mouse and guinea-pig neocortical neurones in slices. *J Physiol* 493(Pt 1):83–97
- Freund TF, Buzsaki G (1996) Interneurons of the hippocampus. *Hippocampus* 6:347–470
- Fuentealba P, Begum R, Capogna M, Jinno S, Marton LF, Csicsvari J, Thomson A, Somogyi P, Klausberger T (2008) Ivy cells: a population of nitric-oxide-producing, slow-spiking GABAergic neurons and their involvement in hippocampal network activity. *Neuron* 57:917–929
- Gulyas AI, Hajos N, Freund TF (1996) Interneurons containing calretinin are specialized to control other interneurons in the rat hippocampus. *J Neurosci* 16:3397–3411
- Gunn BG, Baram TZ (2017) Stress and seizures: space, time and hippocampal circuits. *Trends Neurosci* 40:667–679
- Gunn BG, Cox CD, Chen Y, Frotscher M, Gall CM, Baram TZ, Lynch G (2017) The endogenous stress hormone CRH modulates excitatory transmission and network physiology in hippocampus. *Cereb Cortex* 27:4182–4198

- Haug T, Storm JF (2000) Protein kinase A mediates the modulation of the slow Ca(2+)-dependent K(+) current, I(sAHP), by the neuropeptides CRF, VIP, and CGRP in hippocampal pyramidal neurons. *J Neurophysiol* 83:2071–2079
- Hooper A, Maguire J (2016) Characterization of a novel subtype of hippocampal interneurons that express corticotropin-releasing hormone. *Hippocampus* 26:41–53
- Hooper A, Fuller PM, Maguire J (2018) Hippocampal corticotropin-releasing hormone neurons support recognition memory and modulate hippocampal excitability. *PLoS One* 13:e0191363
- Hu H, Gan J, Jonas P (2014) Interneurons. Fast-spiking, parvalbumin(+) GABAergic interneurons: from cellular design to micro-circuit function. *Science* 345:1255–1263
- Isaacson JS, Scanziani M (2011) How inhibition shapes cortical activity. *Neuron* 72:231–243
- Ivy AS, Rex CS, Chen Y, Dube C, Maras PM, Grigoriadis DE, Gall CM, Lynch G, Baram TZ (2010) Hippocampal dysfunction and cognitive impairments provoked by chronic early-life stress involve excessive activation of CRH receptors. *J Neurosci* 30:13005–13015
- Joels M, Baram TZ (2009) The neuro-symphony of stress. *Nat Rev Neurosci* 10:459–466
- Klausberger T, Somogyi P (2008) Neuronal diversity and temporal dynamics: the unity of hippocampal circuit operations. *Science* 321:53–57
- Klausberger T, Magill PJ, Marton LF, Roberts JD, Cobden PM, Buzsáki G, Somogyi P (2003) Brain-state- and cell-type-specific firing of hippocampal interneurons in vivo. *Nature* 421:844–848
- Klausberger T, Marton LF, Baude A, Roberts JD, Magill PJ, Somogyi P (2004) Spike timing of dendrite-targeting bistratified cells during hippocampal network oscillations in vivo. *Nat Neurosci* 7:41–47
- Kono J, Konno K, Talukder AH, Fuse T, Abe M, Uchida K, Horio S, Sakimura K, Watanabe M, Itoi K (2017) Distribution of corticotropin-releasing factor neurons in the mouse brain: a study using corticotropin-releasing factor-modified yellow fluorescent protein knock-in mouse. *Brain Struct Funct* 222:1705–1732
- Kratzer S, Mattusch C, Metzger MW, Dedic N, Noll-Hussong M, Kafitz KW, Eder M, Deussing JM, Holsboer F, Kochs E, Rammes G (2013) Activation of CRH receptor type 1 expressed on glutamatergic neurons increases excitability of CA1 pyramidal neurons by the modulation of voltage-gated ion channels. *Front Cell Neurosci* 7:91
- Lovett-Barron M, Turi GF, Kaifosh P, Lee PH, Bolze F, Sun XH, Nicoud JF, Zemelman BV, Sternson SM, Losonczy A (2012) Regulation of neuronal input transformations by tunable dendritic inhibition. *Nat Neurosci* 15:423–430, S421–S423
- Madison DV, Nicoll RA (1984) Control of the repetitive discharge of rat CA 1 pyramidal neurones in vitro. *J Physiol* 354:319–331
- Martin EI, Ressler KJ, Jasnow AM, Dabrowska J, Hazra R, Rainnie DG, Nemeroff CB, Owens MJ (2010) A novel transgenic mouse for gene-targeting within cells that express corticotropin-releasing factor. *Biol Psychiatry* 67:1212–1216
- Miles R, Toth K, Gulyas AI, Hajos N, Freund TF (1996) Differences between somatic and dendritic inhibition in the hippocampus. *Neuron* 16:815–823
- Mody I, Pearce RA (2004) Diversity of inhibitory neurotransmission through GABA(A) receptors. *Trends Neurosci* 27:569–575
- Neher E (1992) Correction for liquid junction potentials in patch clamp experiments. *Methods Enzymol* 207:123–131
- Neves G, Cooke SF, Bliss TV (2008) Synaptic plasticity, memory and the hippocampus: a neural network approach to causality. *Nat Rev Neurosci* 9:65–75
- Pawelzik H, Hughes DI, Thomson AM (2002) Physiological and morphological diversity of immunocytochemically defined parvalbumin- and cholecystokinin-positive interneurons in CA1 of the adult rat hippocampus. *J Comp Neurol* 443:346–367
- Pelkey KA, Chittajallu R, Craig MT, Tricoire L, Wester JC, McBain CJ (2017) Hippocampal GABAergic inhibitory interneurons. *Physiol Rev* 97:1619–1747
- Peng J, Long B, Yuan J, Peng X, Ni H, Li X, Gong H, Luo Q, Li A (2017) A quantitative analysis of the distribution of CRH neurons in whole mouse brain. *Front Neuroanat* 11:63
- van den Pol AN (2012) Neuropeptide transmission in brain circuits. *Neuron* 76:98–115
- Refojo D, Schweizer M, Kuehne C, Ehrenberg S, Thoeringer C, Vogl AM, Dedic N, Schumacher M, von Wolff G, Avrabos C, Touma C, Engblom D, Schutz G, Nave KA, Eder M, Wotjak CT, Sillaber I, Holsboer F, Wurst W, Deussing JM (2011) Glutamatergic and dopaminergic neurons mediate anxiogenic and anxiolytic effects of CRHR1. *Science* 333:1903–1907
- Roux L, Buzsáki G (2015) Tasks for inhibitory interneurons in intact brain circuits. *Neuropharmacology* 88:10–23
- Royer S, Zemelman BV, Losonczy A, Kim J, Chance F, Magee JC, Buzsáki G (2012) Control of timing, rate and bursts of hippocampal place cells by dendritic and somatic inhibition. *Nat Neurosci* 15:769–775
- Sarkar J, Wakefield S, MacKenzie G, Moss SJ, Maguire J (2011) Neurosteroidogenesis is required for the physiological response to stress: role of neurosteroid-sensitive GABAA receptors. *J Neurosci* 31:18198–18210
- Stocker M (2004) Ca(2+)-activated K⁺ channels: molecular determinants and function of the SK family. *Nat Rev Neurosci* 5:758–770
- Toth K, Soares G, Lawrence JJ, Philips-Tansey E, McBain CJ (2000) Differential mechanisms of transmission at three types of mossy fiber synapse. *J Neurosci* 20:8279–8289
- Tricoire L, Pelkey KA, Erkkila BE, Jeffries BW, Yuan X, McBain CJ (2011) A blueprint for the spatiotemporal origins of mouse hippocampal interneuron diversity. *J Neurosci* 31:10948–10970
- Walker LC, Cornish LC, Lawrence AJ, Campbell EJ (2018) The effect of acute or repeated stress on the corticotropin releasing factor system in the CRH-IRES-Cre mouse: a validation study. *Neuropharmacology*. <https://doi.org/10.1016/j.neuropharm.2018.09.037> (Epub ahead of print)
- Yan XX, Baram TZ, Gerth A, Schultz L, Ribak CE (1998a) Co-localization of corticotropin-releasing hormone with glutamate decarboxylase and calcium-binding proteins in infant rat neocortical interneurons. *Exp Brain Res* 123:334–340
- Yan XX, Toth Z, Schultz L, Ribak CE, Baram TZ (1998b) Corticotropin-releasing hormone (CRH)-containing neurons in the immature rat hippocampal formation: light and electron microscopic features and colocalization with glutamate decarboxylase and parvalbumin. *Hippocampus* 8:231–243